Supplementary Information (SI) for RSC Advances.
This journal is © The Royal Society of Chemistry 2025

Supporting Information

Synthesis, Radiolabeling, and Biological Evaluation of Methyl 6-deoxy-6-[^{18}F]fluoro-4-thio-α-D-maltotrioside as a PET Bacterial Imaging Agent

Kiyoko Takemiya[a], Wonewoo Seo[b, c], Ronald J. Voll[b, c], Giji Joseph[a], Shelly Wang[a], Fanzing Zeng[b, c], Jonathon A. Nye.[b, c, e], Niren Murthy[d], W. Robert Taylor[a, f, g], and Mark M. Goodman[b, c#]*

a. Division of Cardiology, Department of Medicine, Emory University School of Medicine, 1750 Haygood Dr. NE, Atlanta, Georgia, United States of America, 30322

b. Department of Radiology and Imaging Sciences, School of Medicine, Emory University, 1841 Clifton Road NE, Atlanta, Georgia, United States of America, 30322

c. Center for Systems Imaging, Emory University, 1364 Clifton Rd NE, Atlanta, Georgia, United States of America, 30022

d. Department of Bioengineering, University of California at Berkeley, Berkeley, Stanley Hall 306 California, United States of America, 94720

e. Department of Radiology and Radiological Science, Medical University of South Carolina, 261 Calhoun Street, Charleston, South Carolina, United States of America, 29425

f. Joseph Maxwell Cleland Atlanta VA Medical Center, 1670 Clairmont Road, Decatur, Georgia United States of America, 30033

g. Wallace H. Coulter Department of Biomedical Engineering, School of Medicine, Emory University, 1750 Haygood Dr. NE, Atlanta, Georgia, United States of America, 30322

Corresponding author: Kiyoko Takemiya*, e-mail: kiyoko.takemiya@emory.edu
Co-corresponding author: Mark M. Goodman[#], e-mail: mgoodma@emory.edu

Contents **Pages**

General information. All solvents were purchased from Biosynth, Fisher Scientific or Sigma Aldrich and dried over 4 Å mol sieves (8-12 mesh, Sigma Aldrich). Unless otherwise noted, all commercially available reagents and substrates were used directly as received. Ultra-High Purity dry air was purchased from nexAir LLC. Thin layer chromatography was performed on Merck silica gel plates and visualized by UV light and or H_2SO_4-EtOH. ^{1}H NMR and ^{13}C and ^{19}F NMR spectra were recorded on Varian Mercury 300, Bruker 600, Varian INOVA 600, INOVA 500 and INOVA 400 spectrometers. Residual solvent resonances were treated as internal reference signals. [^{19}F] spectra were referenced to KF. The purification of products was performed via flash chromatography unless otherwise noted. High resolution mass spectra were obtained from the Emory University Mass Spec Facility Inc. The [^{18}F]fluoride was produced at Emory University Center for Systems Imaging with an 11MeV Siemens RDS 111 negative-ion cyclotron (Knoxville, TN) by the [^{18}O](p, n) [^{18}F] reaction using [^{18}O]H_2O (95%). Trap/release cartridges model DW-TRC were purchased from D&W, Inc. (Oakdale, TN). Isolated radiochemical yields were determined using a dose-calibrator (Capintec CRC-712M). Analytical HPLC experiments were performed with a Waters Breeze HPLC system equipped with a Bioscan flow count radioactivity detector and an inline UV detector set to monitor wavelengths 195 nm, 205 nm, and 215 nm (Atlantis T3 column, Waters; mobile phase: 2% EtOH or 3% EtOH). All animal experiments were carried out under humane conditions and were approved by the Institutional Animal Use and Care Committee (IUCAC) and Radiation Safety Committees at Emory University. The purity of all reported compounds is more than 95%, as assessed by ^{1}H NMR, radiometric TLC, or radiometric HPLC, unless otherwise noted.

2. HPLC data

The calibration curve was prepared following procedure: solutions of different volumes of the concentration solutions were injected on the HPLC. Multiplication of injected volume and concentrations of the [^{19}F]MFTMT solutions gave the amount in µmol of injected [^{19}F]MFTMT. The samples were injected to the analytical HPLC and the peak areas were recorded. The calibration curve was plotted using the injected amount (µmol) and peak areas. (Figure S1))

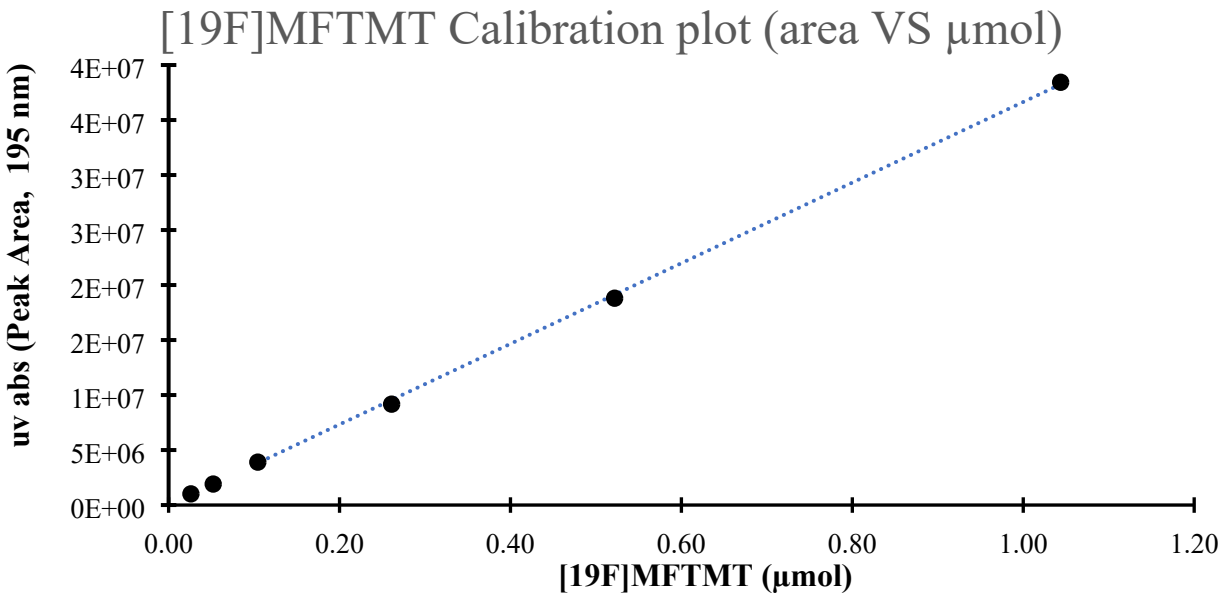

Supplementary Figure S1. [^{19}F]MFTMT Calibration plot. Standard curve of UV absorbance vs amount of [^{19}F]MFTMT is shown. Two of 100 µL of [^{18}F]MFTMT (56.4 mCi/mL @EOB), decayed overnight, samples were injected to the analytical HPLC. The average absorbance was 109285 (±5%), corresponding to 3.0 nmol of [^{19}F]MFTMT. The specific activity of [^{18}F]MFTMT was calculated to be 1.9 Ci/µmol @EOB.

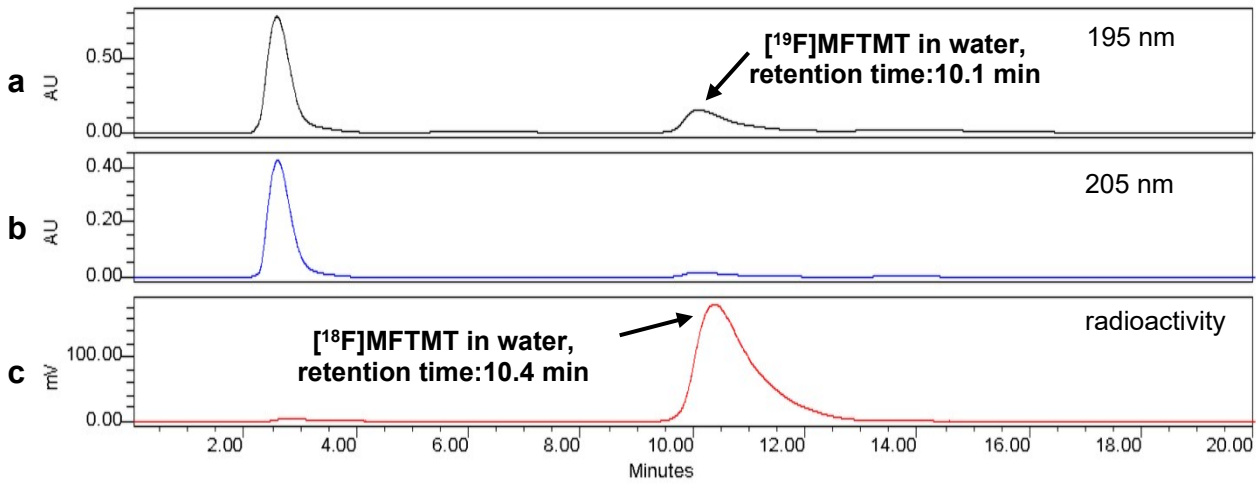

Supplementary Figure S2. Sample chromatograms of the radiometric HPLC analysis of formulated [^{18}F]MFTMT. [^{18}F]MFTMT was identified by co-injection of [^{18}F]MFTMT and non-radiolabeled [^{19}F]MFTMT onto a RT-HPLC system. (a) UV absorbance at 195 nm + co-injection [^{19}F]MFTMT. (b) UV absorbance at 205 nm. (c) [^{18}F]MFTMT radioactivity.

3. ^{1}H, ^{13}C, ^{19}F NMR, & HRMS Spectra:

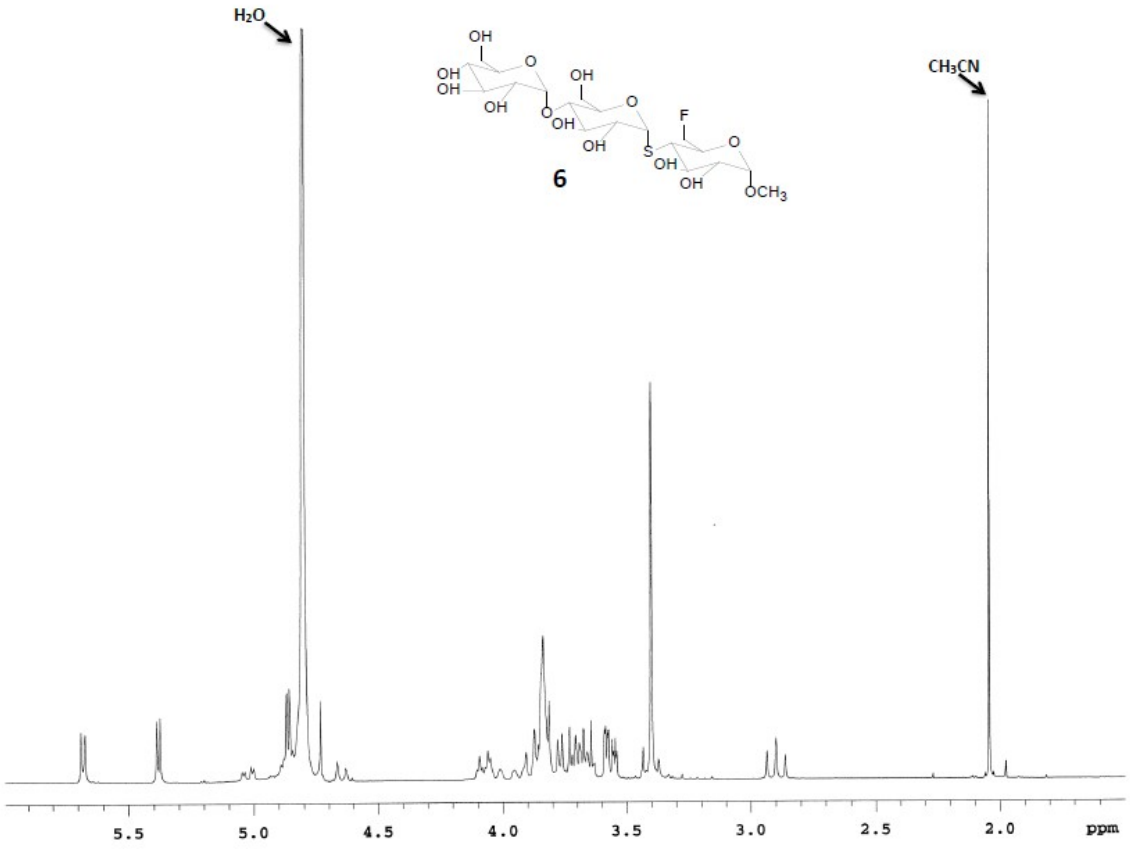

Supplementary Figure S3. ^{1}H NMR [^{19}F]**6** ([^{19}F] MFTMT).

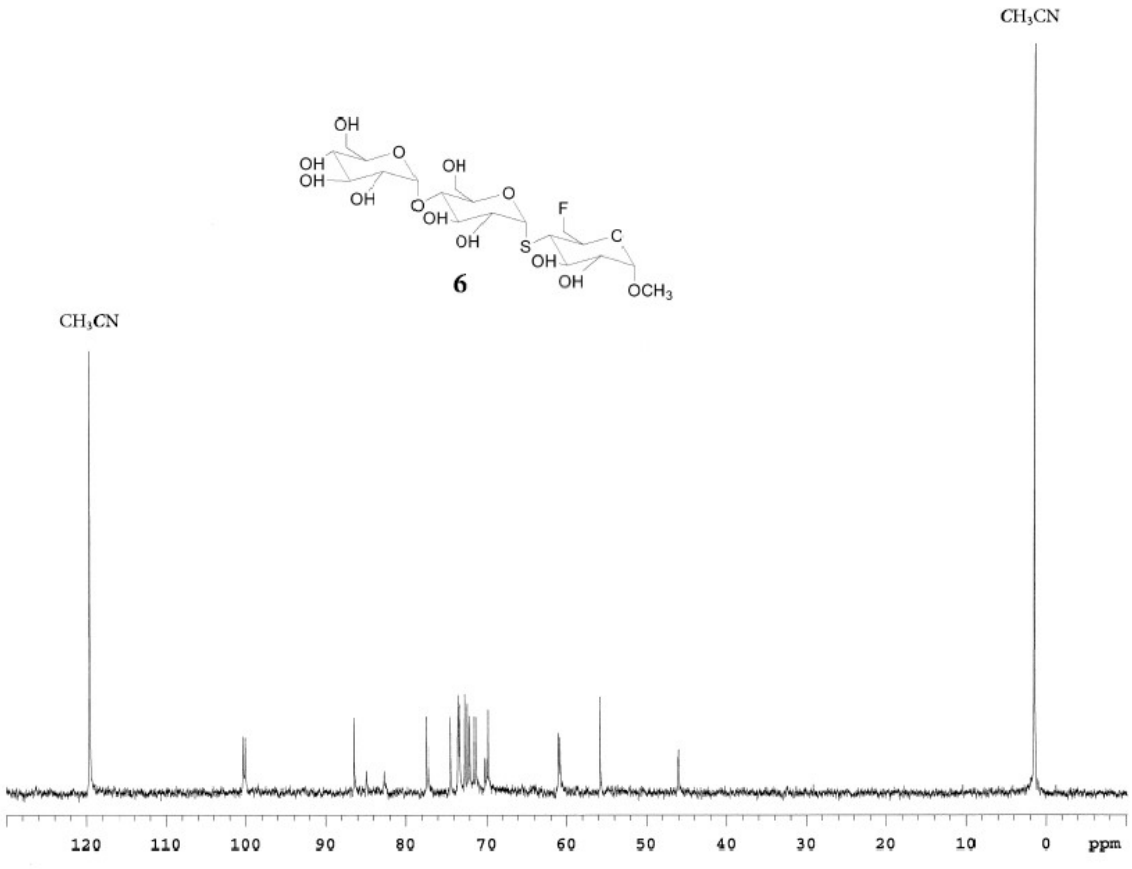

Supplementary Figure S4. ^{13}C NMR [^{19}F]**6** ([^{19}F]MFTMT).

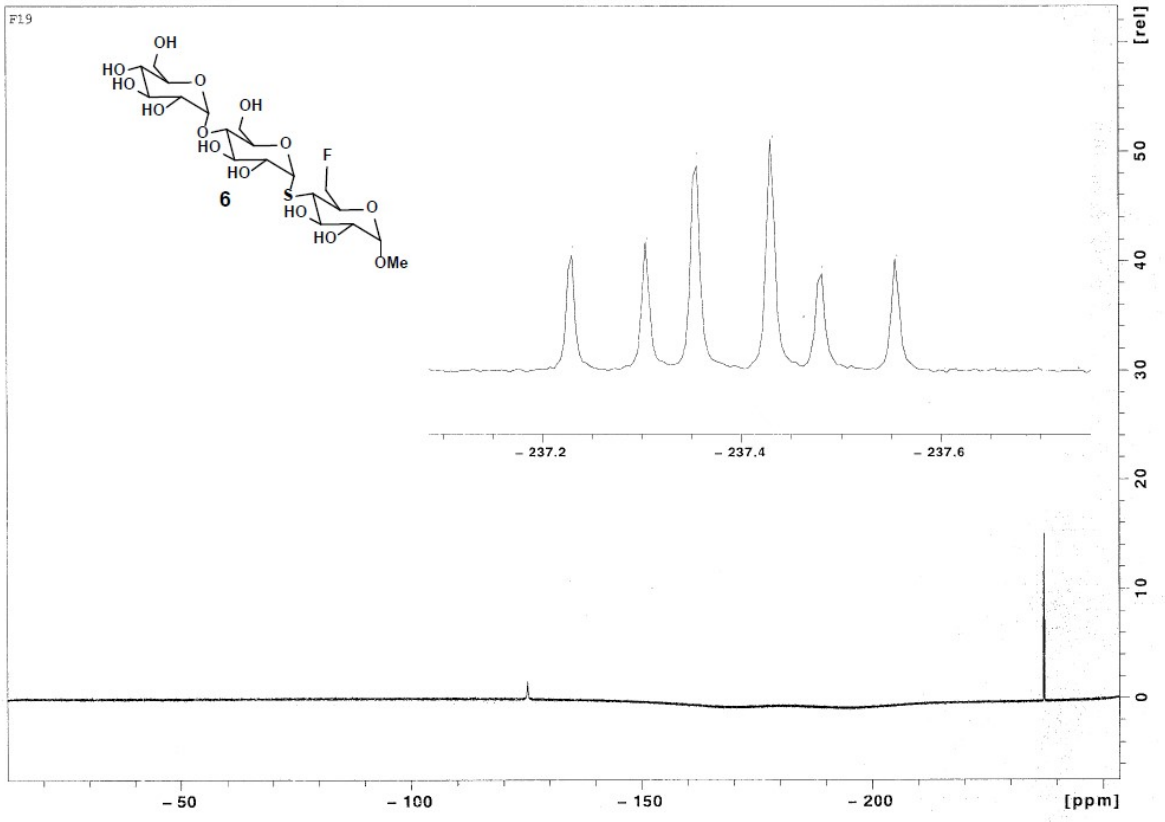

Supplementary Figure S5. ^{19}F NMR [^{19}F]**6** ([^{19}F]MFTMT).

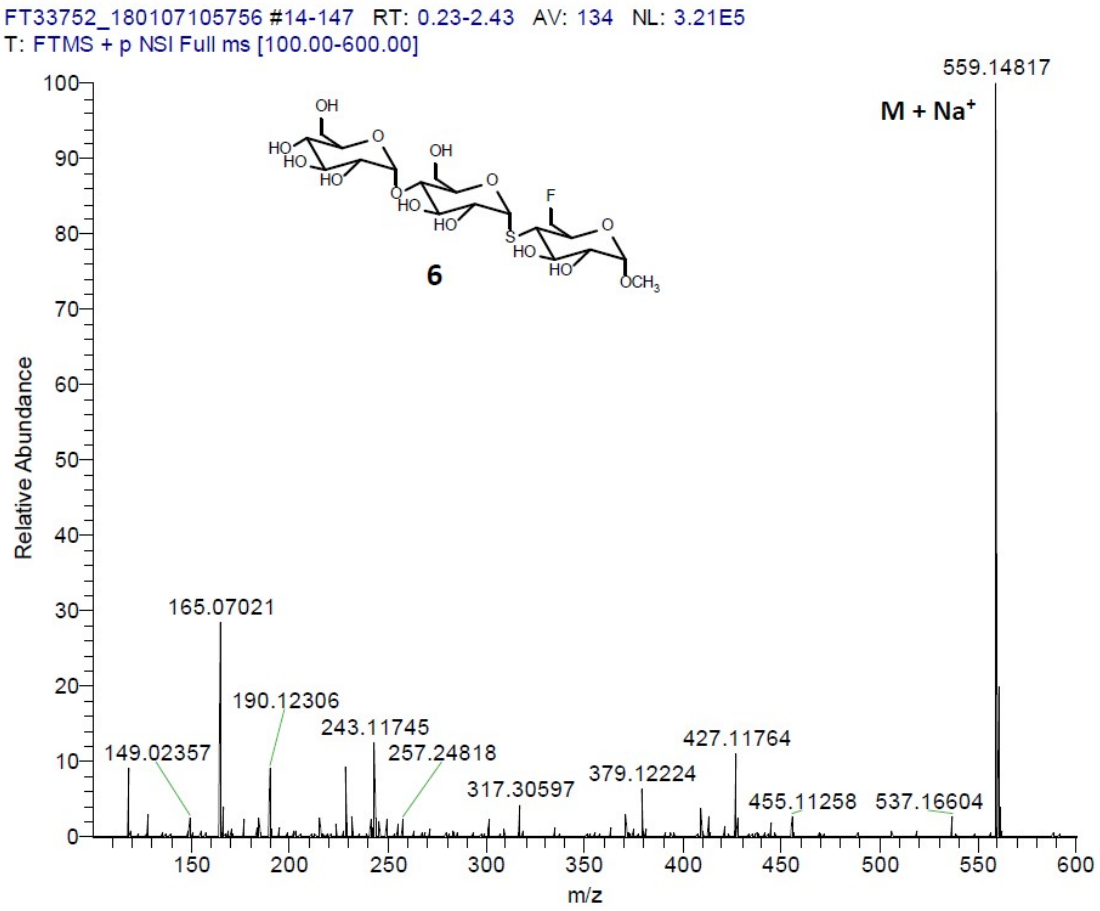

Supplementary Figure S6. HRMS [^{19}F]**6** ([^{19}F]MFTMT).

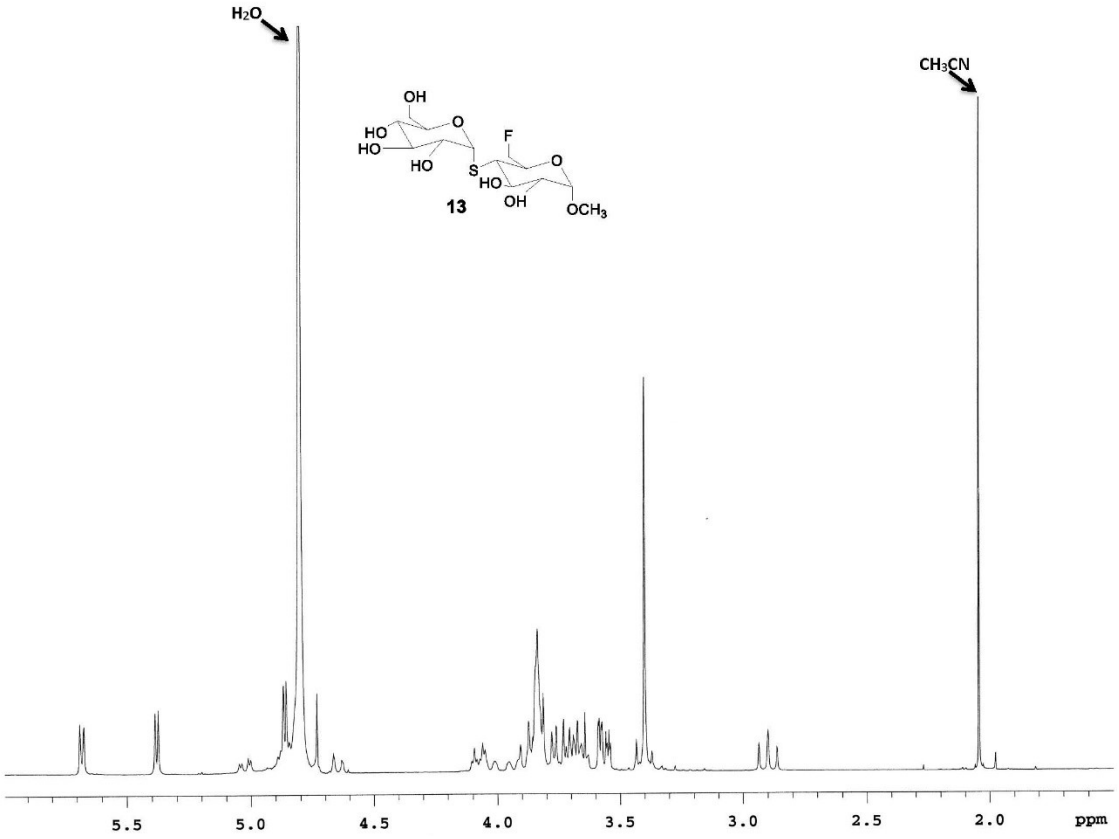

Supplementary Figure S7. ^{1}H NMR [^{19}F]**13** ([^{19}F]MFTM).

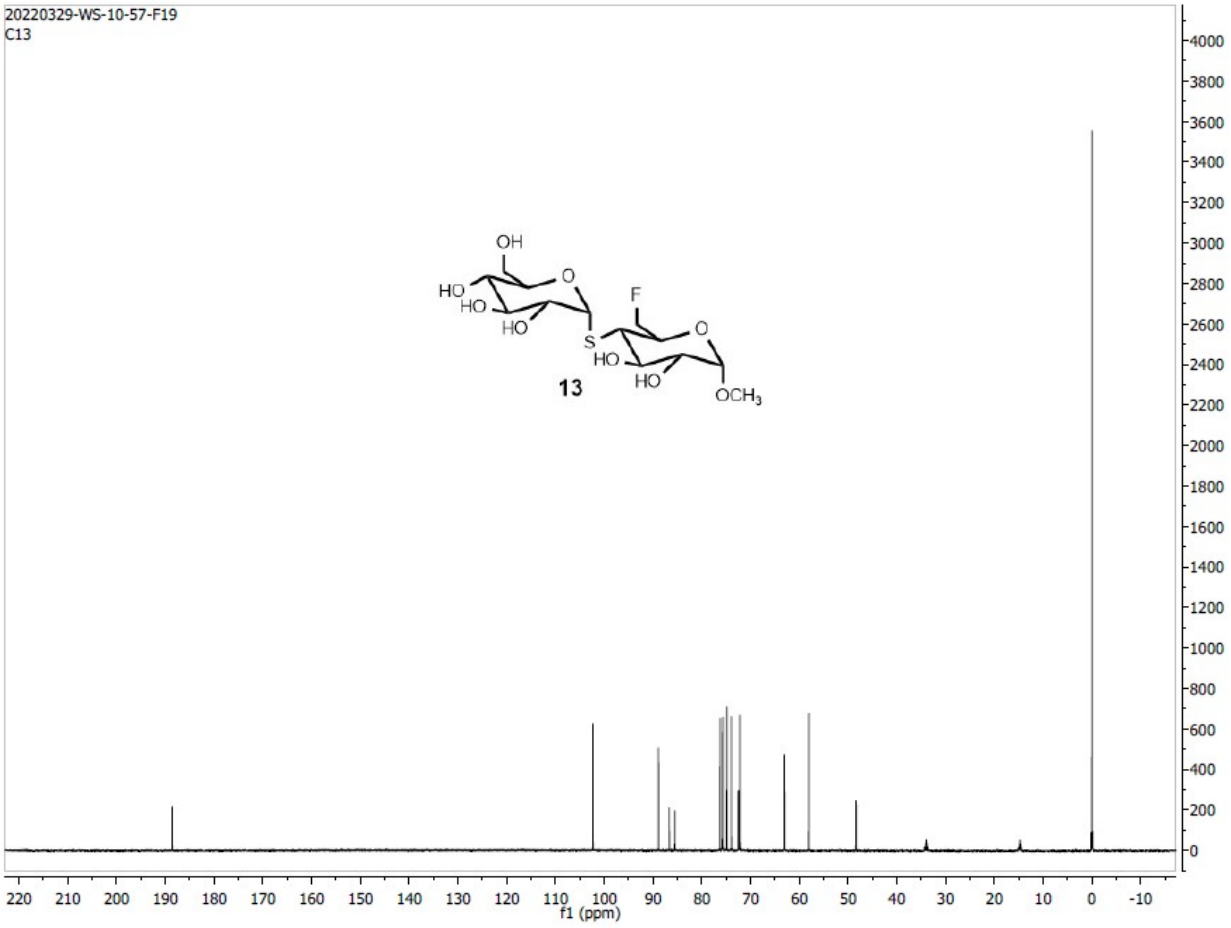

Supplementary Figure S8. ^{13}C NMR [^{19}F]**13** ([^{19}F]MFTM).

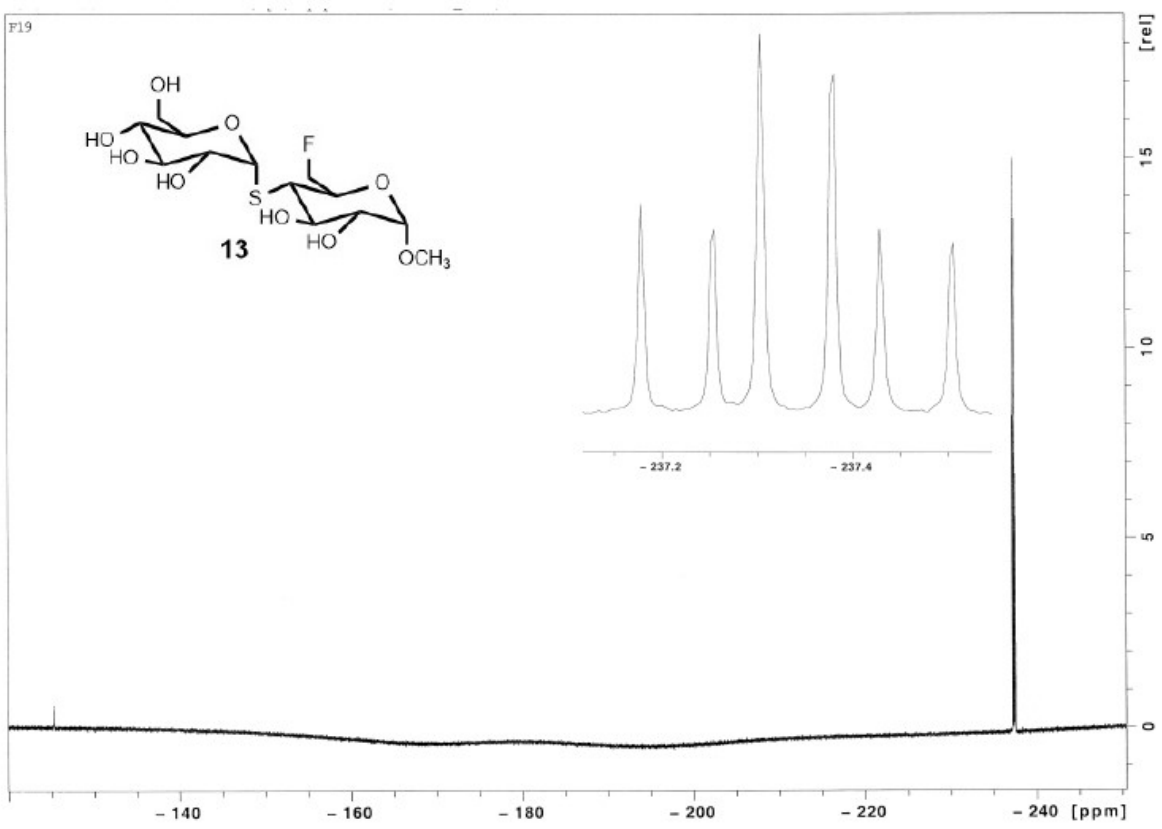

Supplementary Figure S9. ^{19}F NMR [^{19}F]**13** ([^{19}F]MFTM).

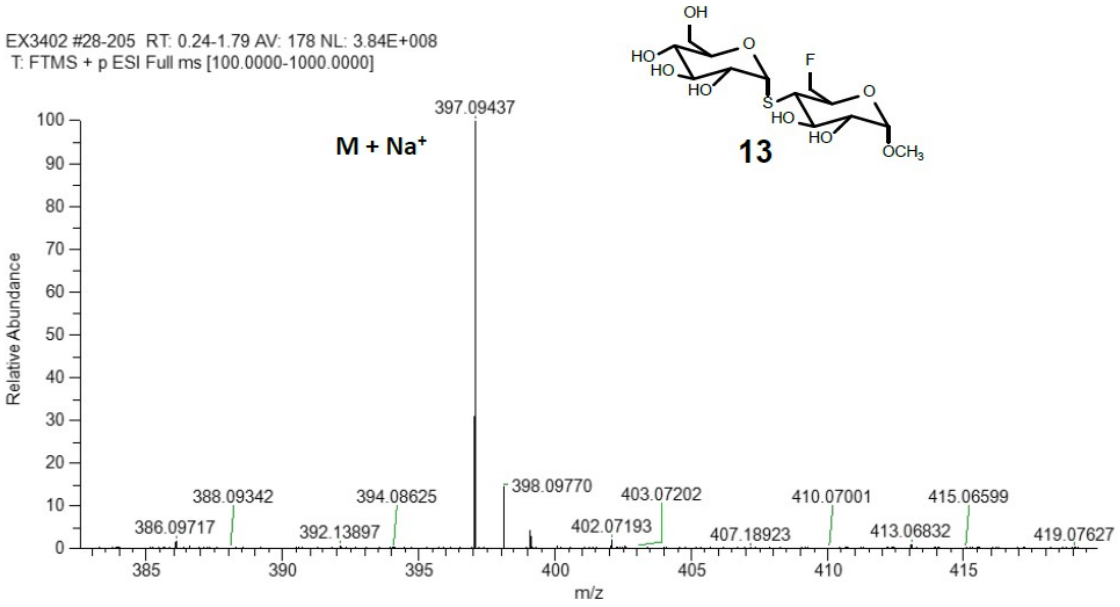

Supplementary Figure S10. HRMS [^{19}F]**13** ([^{19}F]MFTM).

Bacteria	Loading dose (μCi/ml)			
	5	10	15	20
S. aureus	30.9 ± 7.0	65.8 ± 6.0	105.1 ± 4.7	123.8 ± 6.8
E. coli	0.0 ± 0.0	0.3 ± 0.3	1.1 ± 0.5	1.4 ± 0.4
LamB KO *E. coli*	0.0 ± 0.0	1.5 ± 0.7	3.6 ± 2.0	3.2 ± 1.0
CHO-K1 cells	0.0 ± 0.0	0.4 ± 0.3	0.8 ± 0.2	0.9 ± 0.3

Unit: nCi/10^8 CUF

Supplementary Table S1. Uptake of [^{18}F]MFTMT by bacteria and CHO-K1 cells. The bacteria and cells were incubated with 5 to 20 μCi/ml of [^{18}F]MFTMT for 1 h. After washing, the remaining radioactivity was evaluated. The remaining radioactivity in 10^8 CFU of bacteria is shown as nCi. *S. aureus*: *Staphylococcus aureus*, *E.coli*: *Escherichia coli*, LamB KO *E. coli*: LamB knock out *E. coli*.

Bacteria	[^{18}F]MFTMT
E. coli	8.1 ± 1.0
S. aureus	133.3 ± 10.0
LamB KO *E. coli*	7.4 ± 2.7
S. epidermidis	14.9 ± 6.6
P. aeruginosa	10.0 ± 3.5
E. faecalis	2.6 ± 0.3
S. sanguinis	5.7 ± 2.6

Unit: nCi

Supplementary Table S2. Uptake of [^{18}F]MFTMT by pathogenic bacteria. The pathogenic bacteria often found associated with implantable medical device infection were incubated with 20 μCi/ml of [^{18}F]MFTMT or [^{18}F]MFTM for 1 h. After washing, the remaining radioactivity was evaluated. The remaining radioactivity in 10^8 CFU of bacteria is shown as nCi. *E.coli*: *Escherichia coli*, *S. aureus*: *Staphylococcus aureus*, LamB KO *E. coli*: LamB knock out *E. coli*., *S. epidermis*: *Staphylococcus epidermidis*, *P. aeruginosa*: *Pseudononas aeruginosa*, *E. faecalis*, *Enterococcus faecalis*, *S. sanguinis*: *Streptococcus sanguinis*.

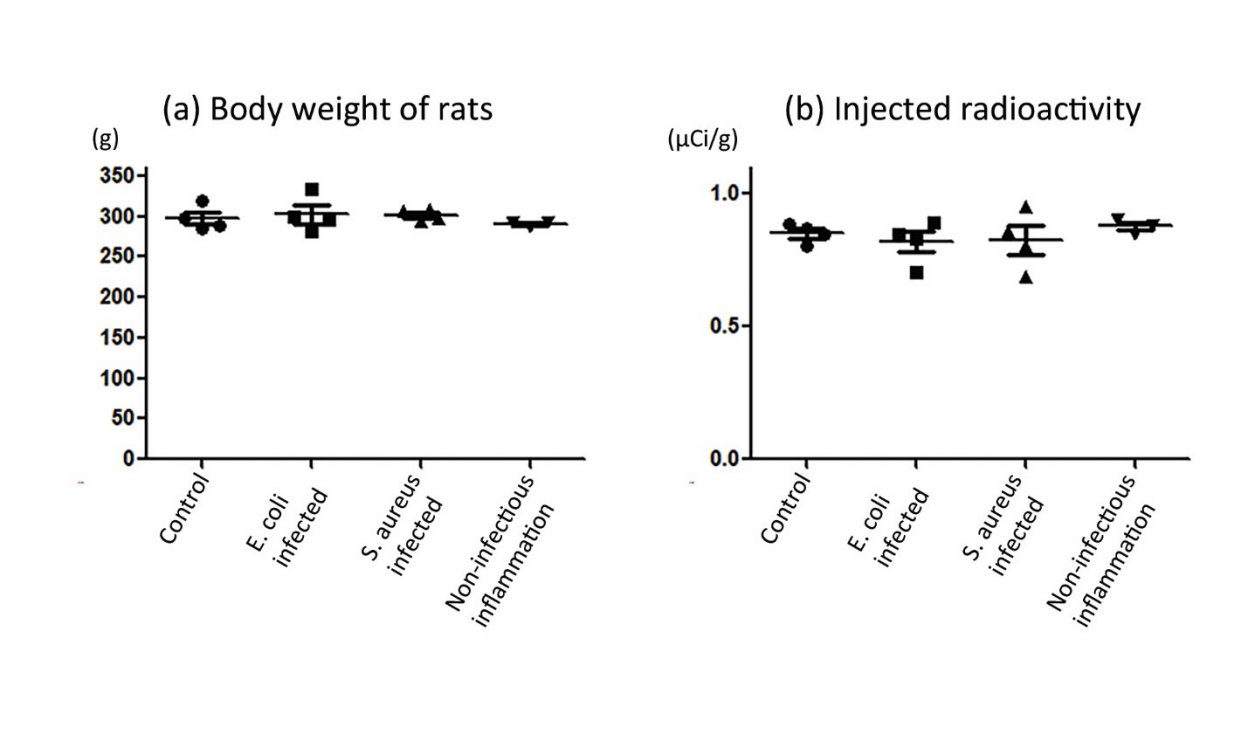

Supplementary Figure S11. The body weights of rats at the time of [^{18}F]MFTMT PET imaging and the intensity of injected radioactivity. (a) The body weights of rats in each group showed no significant differences. (b) The intensity of injected radioactivity was also similar in each group.

a) [^{18}F]MFTMT distribution in control animals.

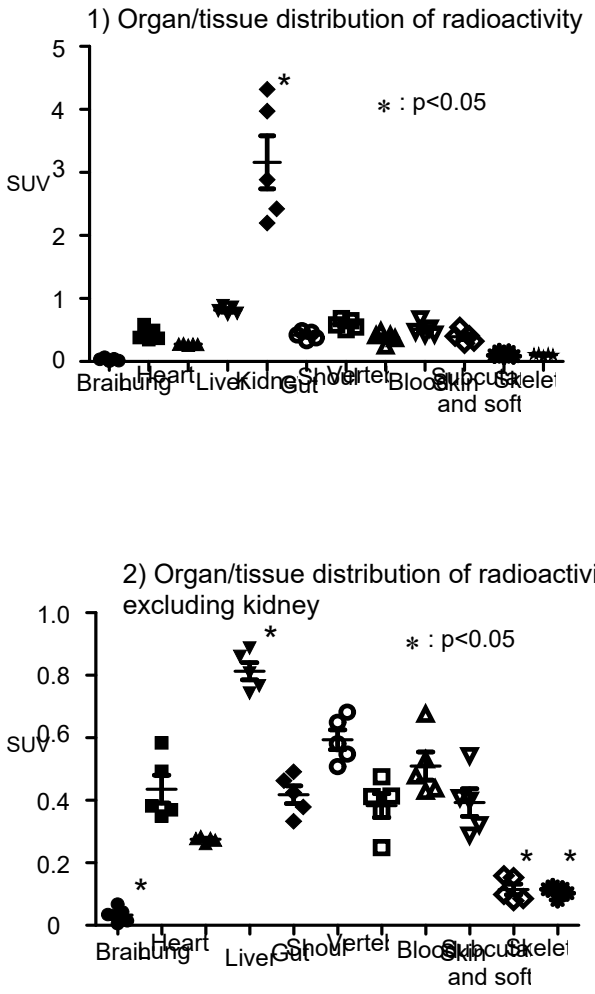

b) [^{18}F]MFTMT PET imaging, coronal and sagittal sections

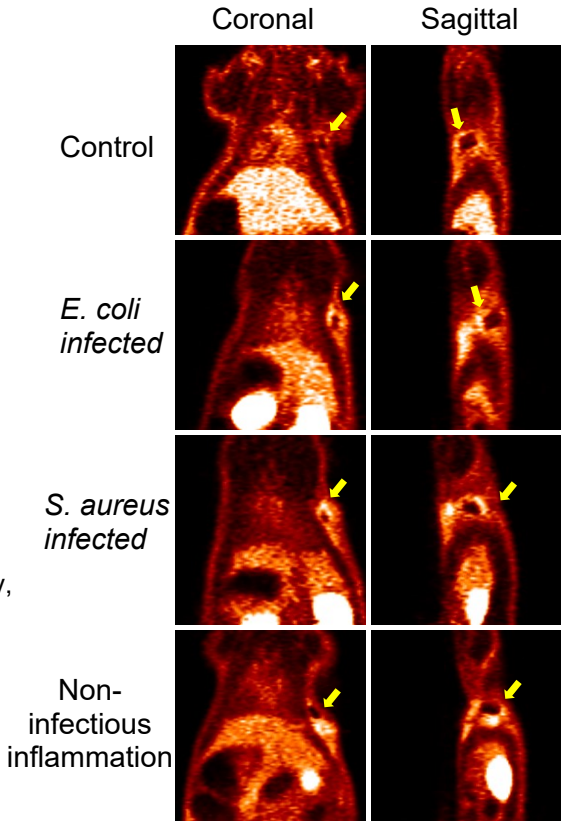

Supplementary Figure S12. In vivo PET imaging with [^{18}F]MFTMT. a) Distribution of radioactivity was evaluated in the control rats. The kidney showed significantly increased accumulation of radioactivity compared with other organs/tissue. When the kidney was excluded, the liver showed an increased accumulation of radioactivity compared with other organs and tissue. In contrast, the brain, subcutaneous fat and soft tissue, and skeletal muscle showed significantly low accumulation of radioactivity compared to the blood. b) [^{18}F]MFTMT PET imaging was conducted on the control, *S. aureus* infected, *E. coli* infected and non-infectious inflammation rats. Transvers sections are shown in the main manuscript. Accumulation of radioactivity was observed in the *S. aureus* infected, *E. coli* infected and non-infectious inflammation rats. (Arrows: mock-ups.)

Groups	SUV mean ratio (A.U.)	SUV max ratio (A.U.)	SUV mean in normal skin (A.U.)	% ID/g tissue in blood (%)
Control	1.36 ± 0.04	2.02 ± 0.18	0.42 ± 0.05	0.18 ± 0.02
E. coli infected	1.85 ± 0.19	2.54 ± 0.21	0.36 ± 0.02	0.16 ± 0.01
S. aureus infected	2.08 ± 0.04	3.000 ± 0.03	0.33 ± 0.04	0.13 ± 0.01
non-infectious inflammation	1.93 ± 0.08	2.65 ± 0.19	0.38 ± 0.06	0.19 ± 0.01

Supplementary Table S3. Analyses of [^{18}F]MFTMT PET imaging in the device infection model in rats. The device infection model rats were scanned with microPET imaging for 60 min after injection of [^{18}F]MFTMT. The imaging data from 30 to 60 min were used for analysis. The accumulation of radioactivity in the reason of interest (ROI) was quantified as the standardized uptake value (SUV), and the accumulation of radioactivity in mock-up areas was compared using the ratio of SUV of the mock-up area to that of the normal skin area. For the analysis of radioactivity in the blood, the retention of radioactivity in the blood is shown as the percentage of injected radioactivity per gram tissue (%ID/g tissue).

Bacteria	Loading dose (μCi/ml)			
	1	5	10	15
S. aureus	19.8 ± 1.2	55.8 ± 11.6	53.4 ± 10.7	41.9 ± 3.3
E. coli	8.0 ± 0.1	8.7 ± 0.1	9.4 ± 0.1	10.3 ± 0.1
LamB KO *E. coli*	8.1 ± 0.2	8.0 ± 0.1	8.3 ± 0.0	8.3 ± 0.1
CHO-K1 cells	0.0 ± 0.0	0.0 ± 0.0	3.0 ± 3.0	9.1 ± 0.2

Unit: nCi/10^8 CFU

Supplementary Table S4. Uptake of serum treated [^{18}F]MFTMT by bacteria and CHO-K1 cells. The bacteria and cells were incubated with 5 to 20 μCi/ml of serum treated [^{18}F]MFTMT for 1 h. After washing, the remaining radioactivity was evaluated. The remaining radioactivity in 10^8 CFU of bacteria is shown as nCi. *S. aureus*: *Staphylococcus aureus*, *E.coli*: *Escherichia coli*, LamB KO *E. coli*: LamB knock out *E. coli*.

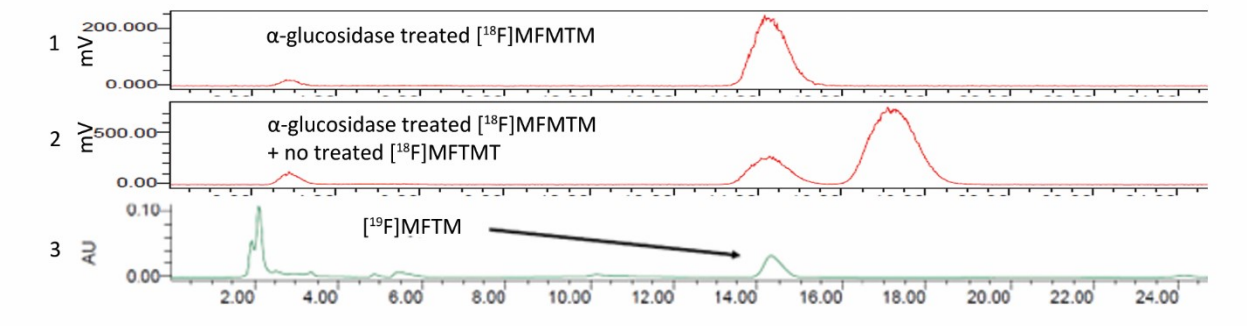

Supplementary Figure S13. HPLC analysis of α-glucosidase treated [^{18}F]MFTMT. [^{18}F]MFTM was generated by digesting [^{18}F]MFTMT by α-glucosidase for 1 h, and the samples were analyzed with radiometric HPLC. (1) α-glucosidase treated [^{18}F]MFTMT, (2) α-glucosidase treated [^{18}F]MFTMT with [^{18}F]MFTMT (Dose), and (3) [^{19}F]MFTM (cold standard). (1) to (3) show that treatment with α-glucosidase generated only [^{18}F]MFTM and no [^{18}F]MFTMT was remained.

Bacteria	[^{18}F]MFTM
E. coli	3.0 ± 0.7
S. aureus	123.1 ± 7.7
LamB KO *E. coli*	7.8 ± 4.8
S. epidermidis	8.0 ± 0.6
P. aeruginosa	7.5 ± 1.3
E. faecalis	2.3 ± 1.4
S. sanguinis	2.6 ± 0.0

Unit: nCi

Supplementary Table S5. Uptake of [^{18}F]MFTM by pathogenic bacteria. The pathogenic bacteria often found associated with implantable medical device infection were incubated with 20 µCi/ml of [^{18}F]MFTMT or [^{18}F]MFTM for 1 h. After washing, the remaining radioactivity was evaluated. The remaining radioactivity in 10^8 CFU of bacteria is shown as nCi. *E.coli*: *Escherichia coli*, *S. aureus*: *Staphylococcus aureus*, LamB KO *E. coli*: LamB knock out *E. coli*., *S. epidermis*: *Staphylococcus epidermidis*, *P. aeruginosa*: *Pseudononas aeruginosa*, *E. faecalis*, *Enterococcus faecalis*, *S. sanguinis*: *Streptococcus sanguinis*.

Cells	inhibitor	[^{18}F]MFTMT	[^{18}F]MFTM
CHO-K1 control	-	1.2 ± 0.0	1.6 ± 0.1
CHO-K1 control	Vehicle	1.5 ± 0.3	1.5 ± 0.1
CHO-K1-hSGLT1	-	4.0 ± 0.1	5.1 ± 0.1
CHO-K1-hSGLT1	Mizagliflozin	2.0 ± 0.1	2.2 ± 0.0
CHO-K1-hSGLT2	-	1.2 ± 0.1	1.9 ± 0.1
CHO-K1-hSGLT2	Dapagliflozin	1.3 ± 0.1	1.7 ± 0.0

Unit: nCi

Supplementary Table S6. Retention of [^{18}F]MFTMT and [^{18}F]MFTM in CHO-K1 cells overexpressing SGLTs. CHO-K1 cells overexpressing human sodium glucose co-transporter (SGLT) 1 or SGLT2 were incubated with 20 μCi/mL of [^{18}F]MFTMT or [^{18}F]MFTM for 1 h, and the radioactivity in the washed cells was evaluated. Some cells were treated with vehicle, mizagliflozin, a specific SGLT1 inhibitor, or dapagliflozin, a specific SGLT2 inhibitor.